2020 IEEE/CIC International Conference on Communications
in China (ICCC)

Indoor CSI fingerprint localization based on tensor decomposition

Yuexin Long
School of Communication and Information Engineering
Chongqing University of posts and Telecommunications
Chongqing, China
longyx98@foxmail.com

Liangbo Xie
School of Communication and Information Engineering
Chongqing University of posts and Telecommunications
Chongqing, China
xielb@cqupt.edu.cn

Mu Zhou
School of Communication and Information Engineering
Chongqing University of posts and Telecommunications
Chongqing, China
zhoumu@cqupt.edu.cn

Yong Wang
School of Communication and Information Engineering
Chongqing University of posts and Telecommunications
Chongqing, China
yongwang@cqupt.edu.cn

***Abstract*—Indoor Wi-Fi localization methods based on the Received Signal Strength (RSS) are widely used because of the low computational complexity and strong applicability. Compared with the RSS, the Channel State Information (CSI) can provide the multi-channel subcarrier phase and amplitude information to better describe the signal propagation path. Thus, the CSI becomes one of the most commonly used signal features in indoor Wi-Fi localization. Compared to the CSI-based geometric localization method, the fingerprint-based localization method has advantages of easy implementation and high accuracy. Based on this, this paper proposes an indoor CSI fingerprint localization approach based on tensor decomposition. Specifically, we combine the tensor decomposition algorithm based on the Parallel Factor (PARAFAC) analysis model with the Alternating Least Squares (ALS) iterative algorithm to reduce the interference of the environment. Then, we use the tensor wavelet decomposition algorithm for feature extraction and obtain the CSI fingerprint. Finally, distinguishing from the traditional localization algorithm based on machine learning, this paper establishes a localization model based on the Partial Least Squares Regression (PLSR) algorithm to predict position coordinates. Experimental results show that the proposed approach is with the high localization accuracy and good fingerprint collection efficiency.**

***Index Terms*—Indoor localization, location fingerprint, channel state information, tensor decomposition, partial least square regression**

I. Introduction

With the gradual development of the mobile internet era to the Internet of Things (IoT) era, the Location-based Service (LBS) has become more and more widely used in peoples lives. At present, the Global Positioning System (GPS) [1] and cellular base station-based localization system [2] belong to the two most mature outdoor localization systems. However, due to the obstruction of various obstacles and moving objects in the indoor environment, the satellite signal attenuation is serious, thus making the indoor localization accuracy unsatisfactory. In comparison, the Wi-Fi [3] network has advantages of the low deployment cost, strong environmental adaptability, and wide communication range, and thereby Wi-Fi-based localization methods are widely used to provide accurate and efficient localization services.

With the continuous development of the network technology, CSI data can now be extracted from commercial Wi-Fi devices. The CSI is more robust than the traditional RSS [4] since it contains more fine-grained and diversified physical layer information during signal transmission to better describe the signal propagation path. Geometry-based localization methods include the angle-based localization method and distance-based localization method. The former performs angle statistics for the signal received at each base station with the known position [5]. However, the current commercial Wi-Fi devices are generally not equipped with a large number of antennas. The effectiveness of using the CSI phase information directly affects the accuracy of the localization. The latter calculates the position by measuring the distance between the target and each base station [6], [7]. However, by considering the serious multipath effect in the indoor environment and the shadowing effect, the localization method based on the RSS generally has a large ranging error [8]. Compared to the geometric localization method, the fingerprint localization method has advantages of easy implementation and high accuracy, but as the size of the fingerprint database increases, the training cost and processing complexity of CSI data greatly increase. In view of the above problems, this paper proposes an indoor CSI fingerprint localization approach based on tensor decomposition.

In summary, the contributions of this paper are as follows. In section III.A, first of all, the tensor model is introduced for CSI noise reduction, and meanwhile the feasibility of combining the tensor decomposition algorithm based on the PARAFAC analysis model with the ALS iterative algorithm for data noise reduction is studied. Secondly, the single-layer tensor wavelet decomposition is carried out in three dimensions of the CSI image by using the tensor wavelet decomposition algorithm, and meanwhile wavelet coefficients in each wavelet sub-

component are counted by using the angular second moment, so as to obtain the CSI localization fingerprint. In section III.B, the paper establishes a localization model based on the PLSR algorithm to predict position coordinates. In section IV, we demonstrate the results of CSI image processing and compare the localization errors of different algorithms. The system framework of this paper is shown in Fig.1.

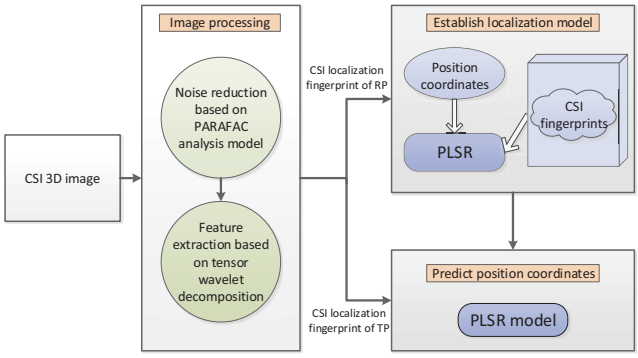

Fig. 1. System architecture.

II. Related Work

Compared to the RSS, the CSI contains more dimensions of information. In addition, in the process of feature extraction, the more feature dimensions indicate the richer location information. In 2017, Zhou et al. [9] proposed a system using SVM classification for device-less detection and location. First, spatial clustering and principal component dimensionality reduction are performed on the CSI data, and then the estimated position is obtained using the SVM algorithm. Zhao et al. [10] proposed a localization system that applied time-domain filtering and dimensionality reduction based on coherent bandwidth to CSI data, and then used an improved kernel-based weighted k-nearest neighbor algorithm for position estimation. Xiao et al. [11] proposed the FIFS, an indoor fingerprint localization system based on the CSI. In this work, the frequency diversity and spatial diversity are processed for the original CSI data, and then a probability model is constructed to map CSI data into fingerprints to obtain the fingerprint database. By considering that the biggest problem with respect to high-dimensional CSI fingerprints is the size of the database, the authors in [12] and [13] proposed to filter out the most relevant feature vectors and reduce dimensions of CSI fingerprints by performing the Principal Component Analysis (PCA) and linear decision analysis respectively.

III. System Model

A. CSI Image Processing

Due to the impact of the environmental noise, the original CSI data need to be de-noised before subsequent feature extraction. According to the previous work in [14], the original CSI data can be represented as a 3-dimensional (3D) image with the X-axis as the subcarrier sequence, Y-axis as the time stamp, and Z-axis as the CSI amplitude.The 3D image is regarded as a third-order tensor $O \in R^{L_1 \times L_2 \times L_3}$, which is represented as

$$O = \sum_{r=1}^{M} \lambda_r \mu_r \circ \upsilon_r \circ \omega_r \tag{1}$$

where $\mu_r \left(\in R^{L_1}\right)$, $\upsilon_r \left(\in R^{L_2}\right)$ and $\omega_r \left(\in R^{L_3}\right)$ are unit vectors obtained by the decomposition of the r-th $(r = 1, \ldots, M)$ rank-1 tensor in three dimensions of the image, the symbol "$\circ$" represents the vector outer product operation, λ_r is the component singular value of the r-th rank-1 tensor, and M is the number of rank-1 tensors used for refactoring O . Then, the tensor decomposition algorithm based on the PARAFAC analysis model is used to estimate the number of rank-1 tensors (i.e., the decomposition series solution) used in the reconstruction of the noiseless image $S\,(= O - N)$, which is calculated as

$$k = SNR \cdot \prod_{i=1}^{3} I_i \Big/ \prod_{i=1}^{3} K_i \tag{2}$$

where N is the noise of O, SNR is the Signal-to-noise Ratio (SNR), I_i is the size of the i-th dimension, and K_i is the rank of the i-order tensor. Let the shape of the tensor as $[I_1, I_2, I_3]$, and I_i is the number of elements of the i-th dimension.Then we can approximately calculate the signal variance as

$$\sigma^2_{signal} \approx \sum_{i=1}^{I_1} \sum_{j=1}^{I_2} \sum_{k=1}^{I_3} O^2_{i,j,k} \Big/ \left(I_1 \times I_2 \times I_3\right) - \sigma^2_{noise} \tag{3}$$

where the noise variance σ^2_{noise} is set as the minimum value of sliding window statistical original CSI image variance, and express the SNR as

$$SNR = \sigma^2_{signal} / \sigma^2_{noise} \tag{4}$$

Then, the Akaike Information Criterion (AIC) is applied to estimate the value K_i , such that

$$K_i = arg \left\{ \min_{r_i} \left\{ -2 \log \left(A\right)^{(L_i - r_i) N_i} + 2 r_i \left(B\right) \right\} \right\} \tag{5}$$

where $A = \prod_{j=r_i+1}^{L_i} \lambda_j^{\frac{1}{L_i - r_i}} \Big/ \frac{1}{L_i - r_i} \sum_{j=r_i+1}^{L_i} \lambda_j$, $B = 2L_i - r_i$, $\lambda_j \, (j = r_i + 1, ..., L_i)$ are eigenvalues obtained after eigenvalue decomposition of the noisy CSI image in three dimensions, L_i and N_i are the number of rows and columns of the i-order expansion matrix $mat_i O \in R^{L_i \times (L_1 \ldots L_{i-1} L_{i+1} \ldots L_3)}$, and r_i is the dominant eigenvalue, which equals to the rank of the estimated i-order tensor when the function in (5) achieves the minimum. By substituting the obtained result SNR, I_i and K_i into (2), decomposition series solution can be obtained.

In order to make the reconstructed noiseless image as close as possible to the ideal noiseless image $\hat{S}$, the ALS iterative algorithm is used in this paper to carry out collaborative filtering among factor matrices. Let the factor matrices of

three dimensions of the CSI image be $U = [\mu_1, ..., \mu_k]$, $V = [\upsilon_1, ..., \upsilon_k]$ and $W = [\omega_1, ..., \omega_k]$ respectively, the weight matrix is $\Lambda = diag[\lambda_1, ..., \lambda_k]$. Since the three factor matrices are unknown, we initialize U, V and W as the all-one matrix. Then the initial reconstructed noiseless image is expressed as

$$S^0 = \sum_{r=1}^{k} \lambda_r \mu_r \circ \upsilon_r \circ \omega_r \tag{6}$$

Based on the idea of ALS iterative algorithm, the two matrices are fixed to solve the remaining matrix. At this point, when different matrix among U, V and W are remained, the 1-order tensor expansion expressions of $\hat{S}$ are $mat_1\hat{S}|_U = U\Lambda(V \bullet W)^T$, $mat_1\hat{S}|_V = V\Lambda(U \bullet W)^T$ and $mat_1\hat{S}|_W = W\Lambda(U \bullet V)^T$. Then, the weighted factor matrices U^*, V^* and W^* are expressed as

$$U^* = mat_1\hat{S}|_U \cdot \left(V^T V \cdot W^T W\right)^{-1} \cdot (V \bullet W)^T \tag{7}$$

$$V^* = mat_1\hat{S}|_V \cdot \left(U^T U \cdot W^T W\right)^{-1} \cdot (U \bullet W)^T \tag{8}$$

$$W^* = mat_1\hat{S}|_W \cdot \left(U^T U \cdot V^T V\right)^{-1} \cdot (U \bullet V)^T \tag{9}$$

where the symbol "$\bullet$" represents the Khatri-Rao product operation of the matrix. We modify factor matrix in each dimension into

$$U_{(i)} = U^*_{(i)} \Big/ \left\| U^*_{(i)} \right\| \tag{10}$$

$$V_{(i)} = V^*_{(i)} \Big/ \left\| V^*_{(i)} \right\| \tag{11}$$

$$W_{(i)} = W^*_{(i)} \Big/ \left\| W^*_{(i)} \right\| \tag{12}$$

where the subscript "(i)" represents the i-th $(i = 1, ..., k)$ column vector in the matrix and the symbol "$\|\|$" represents the norm of the matrix. Then, the column vectors of modified factor matrices are used to reconstruct the noise reduction result of the t-th iteration as

$$S^t = \sum_{r=1}^{k} \lambda_r \mu_r^t \circ \upsilon_r^t \circ \omega_r^t \tag{13}$$

By calculating the difference between the noise reduction results in every two adjacent iterations, we obtain $Err(t) = \left\| S^t - S^{t-1} \right\|$. Here, when the convergence requirement is not met (i.e., $Err(t) = \left\| S^t - S^{t-1} \right\| \geq \varepsilon$), the iteration continues, and otherwise the ideal noiseless image estimation is obtained as $\hat{S} = S^t$. After that, the tensor wavelet decomposition algorithm is used to decompose $\hat{S}$ in three dimensions. The relationship between $\hat{S}$ and the high and low frequency components obtained by tensor wavelet decomposition is expressed as

$$\begin{aligned} \hat{S}^{(X,Y,Z)} &= \left(L^X \oplus H^X\right) \otimes \left(L^Y \oplus H^Y\right) \otimes \left(L^Z \oplus H^Z\right) \\ &= L^X L^Y L^Z \oplus L^X L^Y H^Z \oplus L^X H^Y L^Z \oplus L^X H^Y H^Z \\ &\oplus H^X L^Y L^Z \oplus H^X L^Y H^Z \oplus H^X H^Y L^Z \oplus H^X H^Y H^Z \end{aligned} \tag{14}$$

where symbols "$\oplus$" and "$\otimes$" represent the direct sum operation and the Kronecker product operation of the tensor respectively, L and H represent low-pass and band-pass filters of one-dimensional discrete wavelets acting in three dimensions X, Y and Z.

Denoting eight wavelet sub-components as LLL, LLH, LHL, LHH, HLL, HLH, HHL and HHH respectively. Set the space size of the global data block as $l \times w \times h$, the Angular Second Moment (ASM) is used to count the wavelet coefficients in the m-th $(m = 1, ..., 8)$ wavelet sub-component after the decomposition of the single-layer tensor wavelet, such that

$$ASM_m = \sum_{i=1}^{l/2} \sum_{j=1}^{w/2} \sum_{k=1}^{h/2} P^2(i, j, k) \tag{15}$$

where $P(i, j, k)$ is the wavelet coefficient at (i, j, k) in the matrix corresponding to wavelet sub-component. The information contained in the tensor wavelet sub-component is proved to provide the category discrimination information [15], so this paper applies it to the construction of the CSI localization fingerprint. Based on this, the CSI fingerprint at the n-th $(n = 1, ..., N_f)$ Reference Point(RP) can be expressed as

$$Finger_n = \{ASM_m^n, m = 1, ..., 8\} \tag{16}$$

where N_f is the number of RPs and ASM_m^n is the wavelet coefficient of the m-th wavelet component at the n-th RP.

B. Localization Based on PLSR

Based on the PLSR algorithm, we take the CSI fingerprint $Finger_n = \{ASM_m^n, m = 1, ..., 8\}$ and the position coordinate (x_n, y_n) as independent and dependent variables to establish the localization model. There are in total N_f sample pairs, in which the original independent and dependent variable data, i.e., X_0 and Y_0, are a $N_f \times 8$ and a $N_f \times 2$ dimension matrices respectively, such that

$$X_0 = \begin{pmatrix} ASM_1^1 & \cdots & ASM_8^1 \\ \vdots & \ddots & \vdots \\ ASM_1^{N_f} & \cdots & ASM_8^{N_f} \end{pmatrix} \tag{17}$$

$$Y_0 = \begin{pmatrix} x_1 & y_1 \\ \vdots & \vdots \\ x_{N_f} & x_{N_f} \end{pmatrix} \tag{18}$$

We perform the standardization(including the processing of subtracting the mean and dividing by the standard deviation) of X_0 and Y_0 to obtain X and Y respectively. Then, set the

first principal component axis vectors of X and Y as a 8×1 matrix w_1 and a 2×1 matrix c_1 , we use w_1 and c_1 to express the first pair of principal components of X and Y as $t_1 = Xw_1$ and $u_1 = Yc_1$. According to the solution of the PLSR, we can formulate that

$$\begin{cases} \text{Maximize}\left\{Cov\left(Xw_1, Yc_1\right)\right\} \\ \text{subject to}: \|w_1\| = 1, \|c_1\| = 1 \end{cases} \tag{19}$$

Then, we apply the Lagrange multiplier in the equation below to calculate w_1 and c_1 , such that

$$L = w_1^T X^T Y c_1 - \frac{\lambda}{2}\left(w_1^T w_1 - 1\right) - \frac{\theta}{2}\left(c_1^T c_1 - 1\right) \tag{20}$$

and then calculate the partial derivation of w_1 and c_1 as

$$\frac{\partial L}{\partial w_1} = X^T Y c_1 - \lambda w_1 = 0 \tag{21}$$

$$\frac{\partial L}{\partial c_1} = Y^T X w_1 - \theta c_1 = 0 \tag{22}$$

Since the objective function $Cov\left(Xw_1, Yc_1\right)$ requires to be the maximum, w_1 and c_1 equal to the unit eigenvectors corresponding to the maximum eigenvalues of symmetric matrices $X^T Y Y^T X$ and $Y^T X X^T Y$ respectively. After that, we substitute w_1 and c_1 into $t_1 = Xw_1$ and $u_1 = Yc_1$ to obtain t_1 and u_1 , and then in order to solve the problem of mapping from X to Y , we construct regression models of X and Y for their corresponding principal components t_1 and u_1 as

$$X = t_1 p_1^T + E_1 \tag{23}$$

$$Y = u_1 q_1^T + G_1 \tag{24}$$

where E_1 and G_1 are residual matrices. By taking E_1 as the new X , G_1 as the new Y, we continue the regression looping back and forth until the number of principal components reaches the upper limit (i.e., the rank of X), the algorithm ends. At this point, X and Y can be expressed by the a principal components as

$$X = t_1 p_1^T + t_2 p_2^T + ... + t_a p_a^T + E_a \tag{25}$$

$$Y = u_1 q_1^T + u_2 q_2^T + ... + u_a q_a^T + G_a \tag{26}$$

Since the relationship between X and Y cannot be established from (25) and (26) directly, now we use the correlation between $t_s (s = 1, ..., a)$ and u_s to change Y to regression modeling of the principal component of X, as follows:

$$Y = t_1 r_1^T + t_2 r_2^T + ... + t_a r_a^T \tag{27}$$

Here, the values $p_s = \frac{X^T t_s}{\|t_s\|^2}$, $q_s = \frac{Y^T u_s}{\|u_s\|^2}$ and $r_s = \frac{Y^T t_s}{\|t_s\|^2}$ are calculate by using the least square method. We rewrite (27) in matrix form as

$$Y = TR^T = XWR^T = XA \tag{28}$$

In this case, (28) is recognized as the regression equation which maps from X to Y , where $A = WR^T = \begin{pmatrix} k_1 & l_1 \\ \vdots & \vdots \\ k_8 & l_8 \end{pmatrix}$ is the coefficient matrix of independent variables, $k_b (b = 1, ..., 8)$ and l_b are independent variable coefficients. When W and R are obtained, the PLSR is used to perform prediction. After collecting the original CSI data at Test Point(TP), we perform noise reduction and feature extraction, and then construct the CSI fingerprint as

$$Finger^* = \{ASM_m^*, m = 1, ..., 8\} \tag{29}$$

Finally, we use (30) to estimate the position coordinate (x^*, y^*) of the TP as

$$\begin{aligned} (x^* \ y^*) &= (ASM_1^* ... ASM_8^*)\, A \\ &= (ASM_1^* ... ASM_8^*)\, WR^T \\ &= (ASM_1^* ... ASM_8^*) \begin{pmatrix} k_1 & l_1 \\ \vdots & \vdots \\ k_8 & l_8 \end{pmatrix} \end{aligned} \tag{30}$$

IV. Experiment

A. Experimental Setup

The experiment is conducted on the 5-th floor of the Yifu Building, as shown in Fig.2. The dimensions of the experimental environment is 56.93 m by 20.08 m. There are in total 9 APs randomly deployed in the environment and also 143 RPs and 20 TPs uniformly marked. In Fig.2, the black dots and red triangles represent RPs and TPs respectively. The original CSI data from each AP are collected at each RP, in which the CSI amplitude of 55 available subcarriers are selected for the testing.

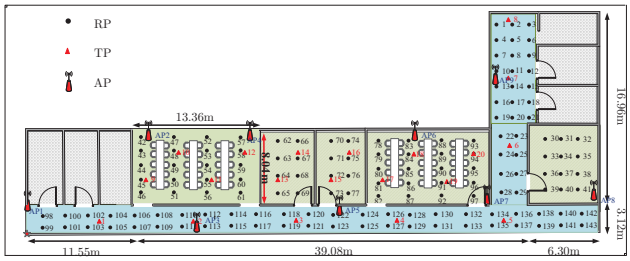

Fig. 2. Experimental environment.

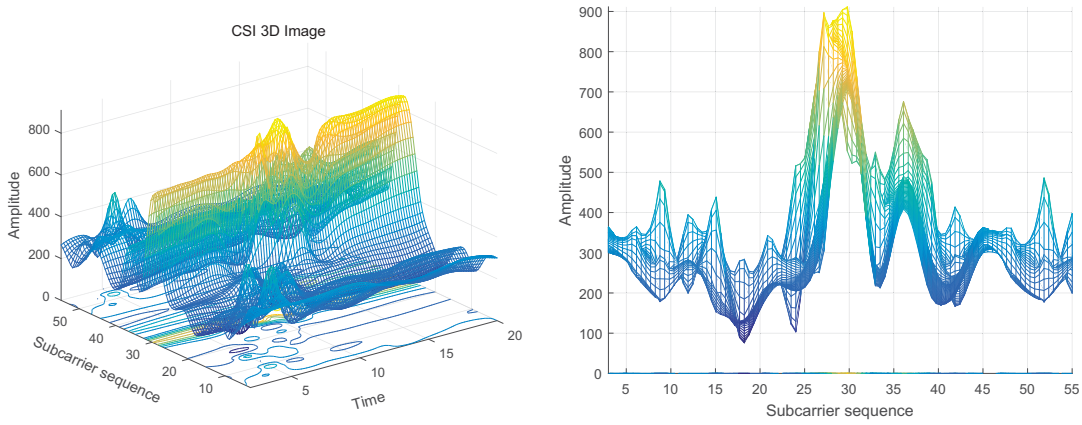

(a) Original CSI 3D image. (b) Original CSI cutaway.

Fig. 3. Original CSI image.

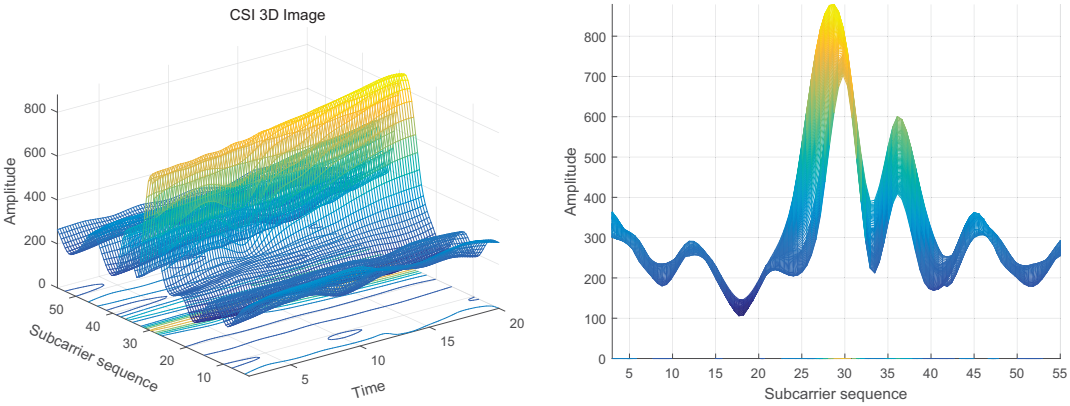

(a) Processed CSI 3D image. (b) Processed CSI cutaway.

Fig. 4. Processed CSI image.

B. Experimental Results

The training samples collected at RPs are used to establish the PLSR localization model, and then the test samples collected at TPs are substituted into this model to obtain the predicted position coordinates. The collected original CSI data is drawn as a 3D image with the corresponding cutaway shown in Fig.3, from which we can find that the original CSI data is affected by the environmental noise. To address this problem, this paper combines the tensor decomposition algorithm based on the PARAFAC analysis model with the ALS iterative algorithm to perform noise reduction on the original CSI data, and then constructs the ideal CSI noiseless image, as shown in Fig.4.

After obtaining the ideal CSI noiseless image, we use the tensor wavelet decomposition algorithm to perform single-layer tensor wavelet decomposition in three dimensions of the CSI image, rely on the ASM to calculate wavelet coefficients of each wavelet sub-component, and then construct the CSI localization fingerprint. After that, we establish a localization model based on the PLSR algorithm to predict position coordinates. As shown in Fig.5, compared to other three existing algorithms (i.e., the KNN [16], APIT [17], and BAYES [18]), we can find that the proposed algorithm has advantages in both the localization error and fingerprint collection efficiency.

V. Conclusion

In this paper, we propose an indoor CSI fingerprint localization approach based on tensor decomposition. The feasibility of combining the tensor decomposition algorithm based on the PARAFAC analysis model with the ALS iterative algorithm for data noise reduction processing is verified. The tensor wavelet decomposition algorithm is used to extract features of the CSI image and obtain the CSI localization fingerprint, and also in order to improve the efficiency of fingerprint collection while ensuring the high localization accuracy, a localization model is established based on the PLSR algorithm to predict the position coordinates. Experimental results show that the proposed preprocessing algorithm has a good noise reduction effect on the original CSI data and compared to the existing localization algorithms, the PLSR algorithm has certain advantages in both the localization error and fingerprint

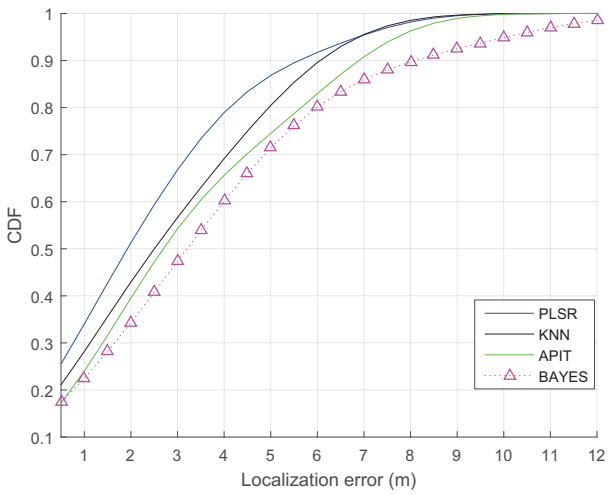

Fig. 5. CDFs of localization errors by different algorithms.

collection efficiency. However, CSI image noise reduction based on Tucker tensor decomposition algorithm forms an interesting work in future. In the next step we will conduct an in-depth study of this algorithm.

REFERENCES

[1] K. Jo, K. Chu and M. Sunwoo, "Interacting Multiple Model Filter-Based Sensor Fusion of GPS With In-Vehicle Sensors for Real-Time Vehicle Positioning," in IEEE Transactions on Intelligent Transportation Systems, vol. 13, no. 1, pp. 329-343.

[2] J. Schloemann, H. S. Dhillon and R. M. Buehrer, "Toward a Tractable Analysis of Localization Fundamentals in Cellular Networks," in IEEE Transactions on Wireless Communications, vol. 15, no. 3, pp. 1768-1782.

[3] M.Liu and J.Sun , "Design and implementation of WLAN indoor positioning system model based on energy efficiency," Chinese Journal of Scientific Instrument, 2014, pp. 1169-1178.

[4] Q. Song, S. Guo, X. Liu, and et al, "CSI Amplitude Fingerprinting-Based NB-IoT Indoor Localization," in IEEE Internet of Things Journal, vol. 5, no. 3, pp. 1494-1504.

[5] A.Cidronali, S. Maddio, G. Giorgetti, and et al, "Analysis and Performance of a Smart Antenna for 2.45-GHz Single-Anchor Indoor Positioning," in IEEE Transactions on Microwave Theory and Techniques, vol. 58, no. 1, pp. 21-31.

[6] Y.Wang, S. Ma and C. L. P. Chen, "TOA-Based Passive Localization in Quasi-Synchronous Networks," in IEEE Communications Letters, vol. 18, no. 4, pp. 592-595.

[7] K.Y. Ng, and et al, "An effective signal strength-based wireless location estimation system for tracking indoor mobile users," Journal of Computer and System Sciences , vol. 79, no. 7, pp. 1005-1016.

[8] L. Gui, M. Yang, H. Yu, and et al, "A CramerCRao Lower Bound of CSI-Based Indoor Localization," in IEEE Transactions on Vehicular Technology, vol. 67, no. 3, pp. 2814-2818.

[9] R. Zhou, J. Chen, X. Lu, and et al, "CSI fingerprinting with SVM regression to achieve device-free passive localization," 2017 IEEE 18th International Symposium on A World of Wireless, Mobile and Multimedia Networks (WoWMoM), Macau, 2017, pp. 1-9.

[10] L. Zhao, H. Wang, P. Li, and et al, "An improved WiFi indoor localization method combining channel state information and received signal strength," 2017 36th Chinese Control Conference (CCC), Dalian, 2017, pp. 8964-8969.

[11] J. Xiao, K.Wu, and et al, "FIFS: Fine-Grained Indoor Fingerprinting System," 2012 21st International Conference on Computer Communications and Networks (ICCCN), Munich, 2012, pp. 1-7.

[12] S. Shi, S. Sigg, L. Chen, and et al, "Accurate Location Tracking From CSI-Based Passive Device-Free Probabilistic Fingerprinting," in IEEE Transactions on Vehicular Technology, vol. 67, no. 6, pp. 5217-5230.

[13] W. Kui, S. Mao, X. Hei, and et al, "Towards Accurate Indoor Localization Using Channel State Information," 2018 IEEE International Conference on Consumer Electronics-Taiwan (ICCE-TW), Taichung, 2018, pp. 1-2.

[14] P. Chen, F. Liu, S. Gao, and et al, "Smartphone-Based Indoor Fingerprinting Localization Using Channel State Information," in IEEE Access, vol. 7, pp. 180609-180619.

[15] Y. Qian, M. Ye and J. Zhou, "Hyperspectral Image Classification Based on Structured Sparse Logistic Regression and Three-Dimensional Wavelet Texture Features," in IEEE Transactions on Geoscience and Remote Sensing, vol. 51, no. 4, pp. 2276-2291.

[16] S. Zhang, X. Li, M. Zong, and et al, "Efficient kNN Classification With Different Numbers of Nearest Neighbors," in IEEE Transactions on Neural Networks and Learning Systems, vol. 29, no. 5, pp. 1774-1785.

[17] Y. Zhang and Q. Zhang, "Research on APIT localization algorithm in wireless sensor networks," 2018 Chinese Control And Decision Conference (CCDC), Shenyang, 2018, pp. 5487-5491.

[18] Z. Wu, Q. Xu, J. Li, and et al, "Passive Indoor Localization Based on CSI and Naive Bayes Classification," in IEEE Transactions on Systems, Man, and Cybernetics: Systems, vol. 48, no. 9, pp. 1566-1577.